Inner Retinal Oxygen Extraction Fraction in Rat

Pang-yu Teng, Justin Wanek, Norman P. Blair, and Mahnaz Shahidi

Purpose. Oxygen extraction fraction (OEF), defined by the ratio of oxygen consumption to delivery, may be a useful parameter for assessing the retinal tissue status under impaired circulation. We report a method for measurement of inner retinal OEF in rats under normoxia and hypoxia based on vascular oxygen tension (PO_2) imaging.

Methods. Retinal vascular PO_2 measurements were obtained in 10 rats, using our previously developed optical section phosphorescence lifetime imaging system. Inner retinal OEF was derived from retinal vascular PO_2 measurements based on Fick's principle. Measurements of inner retinal OEF obtained under normoxia were compared between nasal and temporal retinal sectors and repeatability was determined. Inner retinal OEF measurements obtained under normoxia and hypoxia were compared.

Results. Retinal vascular PO_2 and inner retinal OEF measurements were repeatable (ICC $\geq$ 0.83). Inner retinal OEF measurements at nasal and temporal retinal sectors were correlated ($R = 0.71$; $P = 0.02$; $n = 10$). Under hypoxia, both retinal arterial and venous PO_2 decreased significantly as compared with normoxia ($P < 0.001$; $n = 10$). Inner retinal OEF was 0.46 $\pm$ 0.13 under normoxia and increased significantly to 0.67 $\pm$ 0.16 under hypoxia (mean $\pm$ SD; $P < 0.001$; $n = 10$).

Conclusions. Inner retinal OEF is a promising quantitative biomarker for the adequacy of oxygen supply for metabolism under physiologically and pathologically altered conditions. (*Invest Ophthalmol Vis Sci.* 2013;54:647–651) DOI:10.1167/iovs.12-11305

The maintenance of retinal tissue requires adequate delivery of oxygen by the retinal and choroidal circulations. Indeed, under a severe hypoxic or ischemic insult, retinal function is compromised[1–3] and irreversible functional loss can occur shortly following retinal vascular nonperfusion.[2,4,5] Consequently, it would be advantageous to assess the status of the retina when impaired circulation is suspected.

Oxygen extraction fraction (OEF) is a parameter defined by the ratio of oxygen consumption (MO_2) to oxygen delivery (DO_2). Cerebral OEF measured by positron emission tomography and magnetic resonance imaging has been widely accepted as a valuable parameter for assessing tissue ischemia.[6–13] In fact, increased cerebral OEF, also termed "misery perfusion," has been reported in subjects with acute ischemic stroke[10–12] and carotid occlusion.[7,8] Moreover, an increase in cerebral OEF has been shown to be an independent predictor of stroke.[9,13]

Due to similarities between cerebral and retinal tissues, measurement of OEF may also be useful for assessment of ischemia that occurs in many retinal diseases; however, currently available brain imaging modalities lack adequate resolution to quantify OEF in the retinal tissue. Alternatively, OEF can be expressed as the ratio of the arteriovenous oxygen content difference to the arterial oxygen content based on Fick's principle,[14] as shown by the following equation.

$$\begin{aligned} \text{OEF} &= \frac{MO_2}{DO_2} \\ &= \frac{\text{Blood Flow} \cdot \text{Arteriovenous } O_2 \text{ Content Difference}}{\text{Blood Flow} \cdot \text{Arterial } O_2 \text{ Content}} \\ &= \frac{\text{Arteriovenous } O_2 \text{ Content Difference}}{\text{Arterial } O_2 \text{ Content}} \end{aligned} \quad (1)$$

Therefore, inner retinal OEF can be derived without direct measurements of MO_2 and DO_2.

In the current study, we report a method for quantitative measurement of inner retinal OEF based on retinal vascular oxygen tension (PO_2) imaging.[15] The repeatability, spatial variation, and hypoxia-induced alterations of inner retinal OEF measurements were determined.

Methods

Animals

Ten Long Evans pigmented rats (weight 444 $\pm$ 99 g, mean $\pm$ SD) were used in this study. The rats were treated in compliance with the ARVO Statement for the Use of Animals in Ophthalmic and Vision Research. Anesthesia was induced by intraperitoneal injections of ketamine (100 mg·kg^{-1}) and xylazine (5 mg·kg^{-1}), and maintained with supplemental injections of ketamine (20 mg·kg^{-1}) and xylazine (1 mg·kg^{-1}), as needed. The body temperatures of the rats were maintained at 37°C using an animal holder with a copper tubing water heater. A catheter was placed in a femoral artery and connected to a pressure transducer. Blood pressure and heart rate of the rats were monitored with a data acquisition system (Biopac Systems, Goleta, CA) linked to a pressure transducer connected to the catheter.

The rats were mechanically ventilated with room air (21% O_2, normoxia) and then with 10% oxygen (hypoxia) through an endotracheal tube connected to a small animal ventilator (Harvard Apparatus, Inc., South Natick, MA). To verify the physiological condition, arterial blood was drawn from the femoral arterial catheter to measure systemic arterial oxygen tension (P_aO_2), carbon dioxide tension (P_aCO_2), and pH with a blood gas analyzer (Radiometer, Westlake, OH) and also hemoglobin concentration with a hematology system (Siemens, Tarrytown, NY). Animals were maintained normo-

From the Department of Ophthalmology and Visual Sciences, University of Illinois at Chicago, Chicago, Illinois.

Supported by the National Eye Institute, Bethesda, Maryland, EY17918 (MS) and EY01792 (University of Illinois at Chicago), and Research to Prevent Blindness, New York, New York, senior scientific investigator award (MS), and an unrestricted departmental award.

Submitted for publication November 14, 2012; revised December 20, 2012; accepted December 25, 2012.

Disclosure: **P.-Y. Teng**, None; **J. Wanek**, None; **N.P. Blair**, None; **M. Shahidi**, P

Corresponding author: Mahnaz Shahidi, Department of Ophthalmology and Visual Sciences, University of Illinois at Chicago, 1855 West Taylor Street, Chicago, IL 60612; mahnshah@uic.edu.

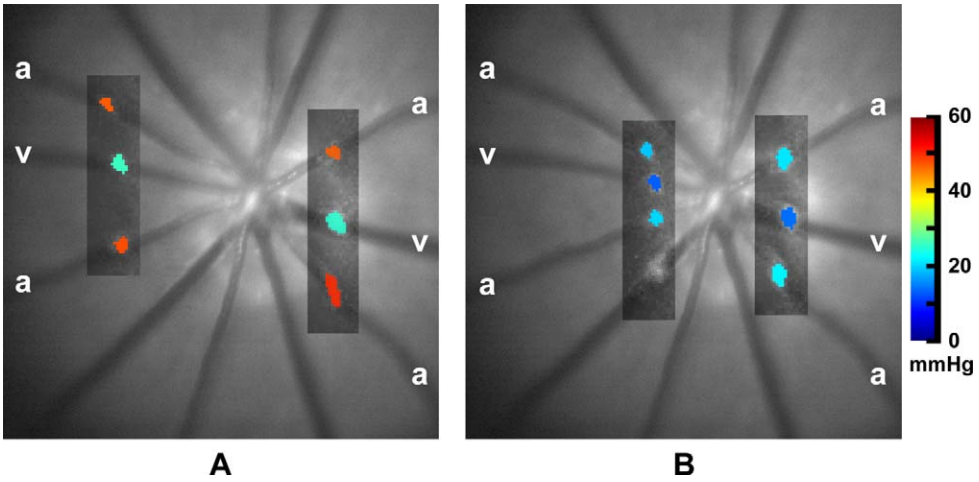

FIGURE 1. Examples of cross-sectional vascular PO_2 maps (*shaded rectangles*) superimposed on red-free retinal images in a rat under normoxia (**A**) and hypoxia (**B**). Maps depict PO_2 in retinal arteries (a) and veins (v) in the temporal (*left*) and nasal (*right*) sides of the optic disc. *Color bar* displays PO_2 in mm Hg.

capnic by adjusting the respiratory minute volume and performing blood gas analysis 5 minutes after each adjustment until P_aCO_2 was within the range of 35 to 45 mm Hg. An oxygen-sensitive molecular probe (Pd-porphine; Frontier Scientific, Logan, UT) was dissolved (12 mg·mL^{-1}) in bovine serum albumin solution (60 mg·mL^{-1}) and administered (20 mg·kg^{-1}) through the femoral arterial catheter, typically 10 minutes prior to imaging. The probe binds to albumin and does not permeate from the normal vasculature to the retinal tissue. The pupils were dilated with 2.5% phenylephrine and 1% tropicamide. Glass cover slips and 1% hydroxypropyl methylcellulose were applied to the corneas to eliminate the refractive power and to prevent dehydration.

Retinal Vascular Oxygen Tension Imaging

Retinal vascular PO_2 was measured with our custom optical section phosphorescence lifetime imaging system.[15] In short, a laser beam was focused to a vertical line, and projected at an oblique angle on the retina. An optical section phosphorescence image of the retinal vasculature was acquired with an intensified charge-coupled device camera attached to a slit lamp biomicroscope. Since the incident laser beam was at an angle with respect to the imaging path, phosphorescence emissions of the Pd-porphine from the retinal vessels were depth-resolved. Phosphorescence lifetime was determined using a frequency-domain approach and converted to PO_2 measurements using the Stern-Volmer relationship defined by $PO_2 = (1/\kappa_Q) \cdot (1/\tau - 1/\tau_0)$, where κ_Q (mm Hg^{-1}·μs^{-1}) is the quenching constant for the triplet-state of Pd-porphine, τ (μs) is the phosphorescence lifetime, and τ_0 (μs) is the lifetime in a zero-oxygen environment.[16,17] Measurements of PO_2 were obtained in a retinal sector, defined by a zone bounded by two major retinal arteries (PO_{2A}), with a major retinal vein (PO_{2V}) between the two arteries (Fig. 1). Three repeated measurements were obtained at nasal and temporal retinal sectors, within three optic disc diameters (~600 μm) from the edge of the optic nerve head. A red-free retinal image was acquired for documenting the locations of the PO_2 measurements. Under both ventilation conditions, the laser power incident on the cornea was approximately 40 μW, which is safe for 1 hour of continuous viewing according to the American National Standard Institute for Safety Standards.[18]

Quantification of OEF

Based on retinal vascular PO_2 measurements, the O_2 content of blood was estimated as follows:

$$O_2 \text{ content} = O_{2max} \cdot Hgb \cdot SO_2 + k \cdot PO_2 \quad (2)$$

where O_{2max} is the maximum oxygen carrying capacity of hemoglobin (1.39 mLO_2·g^{-1}),[19] Hgb is the measured hemoglobin concentration of arterial blood (13.9 ± 0.5 g·dL^{-1}; $n = 10$), k is the oxygen solubility in blood (0.003 mLO_2·dL^{-1}·mm Hg^{-1}),[19] and SO_2 is the oxygen saturation. Based on vascular PO_2 and arterial blood pH measurements, SO_2 was calculated from the Hill equation, which models the oxygen dissociation curve and is defined as $SO_2 = (PO_2/P_{50})^n/(1 + [PO_2/P_{50}]^n)$, where n is an empirical constant taken to be 2.6 in rat,[20] and P_{50} is the PO_2 when SO_2 is 0.5 at a given pH, based on the Bohr effect.[21]

Inner retinal OEF was quantified in a retinal sector as follows,

$$OEF = \frac{mO_{2A} - O_{2V}}{mO_{2A}} \quad (3)$$

where mO_{2A} is the mean arterial O_2 content of the two major arteries, and O_{2V} is the venous O_2 content. The mean arterial PO_2 of the two major arteries (mPO_{2A}) was also calculated.

Data Analysis

Repeatability of mPO_{2A}, PO_{2V}, and OEF was determined by calculating the intraclass correlation coefficients (ICCs) and the SDs of three repeated measurements obtained under normoxia at a retinal sector nasal to the optic disc. Repeated measurements of mPO_{2A}, PO_{2V}, and OEF at each retinal sector were averaged, and spatial variation was assessed by relating OEF measurements at nasal and temporal sectors using Pearson's correlation. In each rat, measurements of mPO_{2A}, PO_{2V}, and OEF at nasal and temporal retinal sectors were averaged, and the mean values under normoxia and hypoxia were compared with paired Student's *t*-test. Statistical significance was accepted at P less than 0.05.

RESULTS

Repeatability and Spatial Variation

The ICCs and mean SDs (averaged over data in 10 rats) obtained from three repeated mPO_{2A}, PO_{2V}, and OEF measurements in nasal retinal sectors under normoxia are shown in Table 1. Measurements of mPO_{2A} and PO_{2V} were repeatable, with ICCs greater than or equal to 0.86 and mean SDs less than or equal to 3 mm Hg. Similarly, inner retinal OEF measurements were also repeatable (ICC = 0.83 and mean SD = 0.08). As anticipated,

Table 1. ICCs and mean SDs, Averaged over Data in 10 Rats, Based on Three Repeated mPO_{2A}, PO_{2V}, and OEF Measurements in the Nasal Sectors under Normoxia

	ICC	SD
mPO_{2A}	0.86	3 mm Hg
PO_{2V}	0.89	2 mm Hg
OEF	0.83	0.08

measurements of OEF at nasal and temporal retinal sectors were correlated under normoxia ($R = 0.71$; $P = 0.02$; $n = 10$).

Systemic Physiological Status

The systemic physiological status of the rats under normoxia and hypoxia is presented in Table 2. P_aO_2 under hypoxia (34 ± 4 mm Hg) was significantly lower as compared with normoxia (93 ± 8 mm Hg) ($P < 0.001$; $n = 10$). Due to controlled ventilation, P_aCO_2 under normoxia and hypoxia were similar ($P = 0.76$). Arterial blood pH, blood pressure, and heart rate decreased significantly under hypoxia ($P \leq 0.001$).

Retinal Vascular PO_2 and OEF

Examples of cross-sectional vascular PO_2 maps obtained in the same rat under normoxia and hypoxia are shown overlaid on the corresponding red-free retinal images in Figure 1. As expected, in both nasal and temporal sectors, mPO_{2A} was higher than PO_{2V} under both normoxia and hypoxia. Both mPO_{2A} and PO_{2V} decreased under hypoxia as compared with normoxia.

Measurements of mPO_{2A} and PO_{2V} averaged over all rats under normoxia and hypoxia are listed in Table 2. Under normoxia, $mPO2_A$ and $PO2_V$ were 44 ± 4 and 28 ± 5 mm Hg, respectively ($n = 10$). Under hypoxia, both mPO_{2A} (20 ± 4 mm Hg) and PO_{2V} (11 ± 4 mm Hg) decreased significantly as compared with normoxia ($P < 0.001$). Mean measurements of inner retinal OEF under normoxia and hypoxia are shown in Figure 2. Mean inner retinal OEF was 0.46 ± 0.13 under normoxia and increased significantly to 0.67 ± 0.16 under hypoxia ($P < 0.001$; $n = 10$).

Discussion

Retinal ischemia is implicated in many retinal diseases that lead to visual impairment; however, methods that can quantitatively assess the retinal tissue status in vivo under ischemia are limited. One potential parameter is OEF, which indicates the adequacy of oxygen supply relative to the tissue's metabolic demand. In the current study, we report for the first time to our knowledge, quantitative measurements of inner retinal OEF in rats based on retinal vascular PO_2 imaging, and demonstrate a significant increase in inner retinal OEF under systemic hypoxia.

Table 2. The Systemic Physiologic Status and Retinal Vascular PO_2 Measurements under Normoxia and Hypoxia

	Normoxia	Hypoxia	*P* Value
Systemic physiologic status			
P_aO_2, mm Hg	93 ± 8	34 ± 4	<0.001*
P_aCO_2, mm Hg	40 ± 5	41 ± 5	0.76
pH	7.38 ± 0.05	7.31 ± 0.05	<0.001*
Blood pressure, mm Hg	113 ± 17	78 ± 22	0.001*
Heart rate, beats·min^{-1}	214 ± 36	162 ± 45	0.002*
Retinal vascular PO_2			
mPO_{2A}, mm Hg	44 ± 4	20 ± 4	<0.001*
PO_{2V}, mm Hg	28 ± 5	11 ± 4	<0.001*

Means and SDs of measurements in 10 rats are listed. Asterisks indicate statistically significant differences between normoxia and hypoxia.

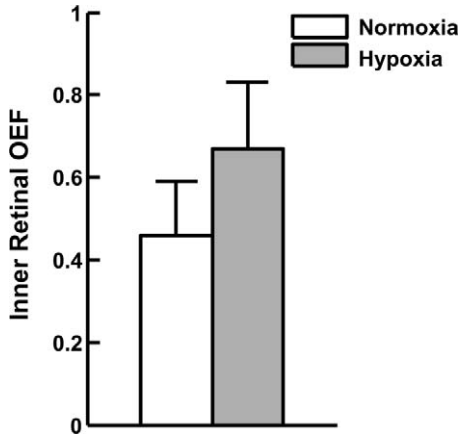

Figure 2. Inner retinal oxygen extraction fraction (OEF) under hypoxia (0.67 ± 0.16) was significantly higher than under normoxia (0.46 ± 0.13) (mean ± SD; $P < 0.001$; $n = 10$).

Inner retinal OEF measurements in the current study were compared with calculated retinal and measured cerebral OEFs due to a lack of published retinal data. Based on oximetry studies in healthy subjects,[22–24] we computed the inner retinal OEF to be 0.40, which is comparable to our measurements of 0.46 in rats under normoxia. Additionally, inner retinal OEF measured under normoxia in the current study was in agreement with published cerebral OEFs (0.37 to 0.57).[25–30] Our finding of increased inner retinal OEF under systemic hypoxia was similar to elevated inner retinal OEF in chronic systemic hypoxia[31] and central retinal vein occlusion,[32] calculated from oximetry data in humans. Moreover, this finding was also consistent with the response of cerebral OEF under hypoxia.[25,27,30]

An increase in inner retinal OEF can occur due to either an increase in retinal MO_2 or a decrease in DO_2. Under hypoxia, because MO_2 is unlikely to increase, the observed increase in inner retinal OEF would occur due to a decrease in DO_2 that can result from reductions in retinal blood flow and/or arterial blood oxygen content. Although retinal blood flow in principle could be affected by systemic blood pressure and/or blood pH, it was not likely influenced by these factors under our experimental conditions. Blood pressure remained within the autoregulatory range,[33] even though it was reduced during hypoxia. Likewise, a change in blood pH was not expected to alter blood flow, according to findings in the brain.[34,35] On the other hand, hypoxia has been reported to increase retinal blood flow,[36–39] which would tend to maintain DO_2. Nevertheless, the compensatory increase in blood flow may not be adequate to maintain DO_2, if the hypoxia is severe enough. In that case, because of reductions in retinal arterial blood oxygen content, DO_2 decreases, thereby causing an increase in inner retinal OEF.

One factor that likely affected our results was that oxygen contents in retinal veins were estimated from the oxygen dissociation curve using the arterial blood pH. Because blood pH is expected to be lower in veins than in arteries,[40,41] the actual venous oxygen contents were likely lower due to a right

shift of the oxygen dissociation curve. As a result, the actual inner retinal OEF should have been higher than the reported values under normoxia. The right shift of the oxygen dissociation curve would be expected to be even more prominent during hypoxia due to increased anaerobic metabolism. Because OEF was underestimated under both ventilation conditions, this limitation likely did not affect our finding of increased inner retinal OEF under hypoxia.

Measurements of inner retinal OEF may provide information about the retinal tissue status during ischemic insult complementary to retinal blood flow measurements or conventional diagnostic tests, such as fundus photography and fluorescein angiography. An acute increase in retinal OEF indicates a state of misery perfusion, in which DO_2 declines, and thereby support for MO_2 becomes precarious. If DO_2 remains reduced chronically, irreversible anoxic damage may develop, leading to decreases in retinal MO_2 and OEF. Therefore, while OEF is elevated, retinal tissue may still remain viable,[42] thus potentially providing a window of opportunity for successful intervention, as has been demonstrated in cerebral tissue.[43–45] In the current study, we evaluated inner retinal OEF under two ventilation conditions to establish a normal baseline and demonstrate a response to a severe hypoxic challenge. Additional studies that assess inner retinal OEF in response to varying levels of inspired oxygen may help establish a threshold at which OEF begins to increase due to maximized blood flow compensation. Furthermore, future studies are needed to provide knowledge of OEF response in experimental animal models of retinal vascular deficiency that may eventually be translated for clinical management of patients.

In summary, we established a method for quantitative measurement of inner retinal OEF in rats and demonstrated an increase in OEF under acute systemic hypoxia. The method can be extended to provide a global assessment of inner retinal OEF by measuring O_2 contents in all major retinal blood vessels. Quantification of inner retinal OEF has potential value for providing information about the retinal energy metabolism under challenged physiological and pathological conditions.

References

1. Linsenmeier RA. Electrophysiological consequences of retinal hypoxia. *Graefes Arch Clin Exp Ophthalmol*. 1990;228:143–150.
2. Osborne NN, Casson RJ, Wood JP, Chidlow G, Graham M, Melena J. Retinal ischemia: mechanisms of damage and potential therapeutic strategies. *Prog Retin Eye Res*. 2004; 23:91–147.
3. Weidner C. The c-wave in the ERG of albino rat. *Vision Res*. 1976;16:753–763.
4. Hayreh SS, Weingeist TA. Experimental occlusion of the central artery of the retina. IV: retinal tolerance time to acute ischaemia. *Br J Ophthalmol*. 1980;64:818–825.
5. Hayreh SS, Zimmerman MB, Kimura A, Sanon A. Central retinal artery occlusion. Retinal survival time. *Exp Eye Res*. 2004;78: 723–736.
6. Baron JC, Jones T. Oxygen metabolism, oxygen extraction and positron emission tomography: historical perspective and impact on basic and clinical neuroscience. *Neuroimage*. 2012;61:492–504.
7. Derdeyn CP. Pet imaging in carotid stenosis. In: Schaller B, ed. *Imaging of Carotid Artery Stenosis*. New York: Springer; 2007:85–102.
8. Derdeyn CP, Grubb RL Jr, Powers WJ. Cerebral hemodynamic impairment: methods of measurement and association with stroke risk. *Neurology*. 1999;53:251–259.
9. Grubb RL Jr, Derdeyn CP, Fritsch SM, et al. Importance of hemodynamic factors in the prognosis of symptomatic carotid occlusion. *JAMA*. 1998;280:1055–1060.
10. Heiss WD, Herholz K. Assessment of pathophysiology of stroke by positron emission tomography. *Eur J Nucl Med*. 1994;21:455–465.
11. Muir KW, Buchan A, von Kummer R, Rother J, Baron JC. Imaging of acute stroke. *Lancet Neurol*. 2006;5:755–768.
12. Powers WJ, Zazulia AR. PET in cerebrovascular disease. *PET Clin*. 2010;5:83106.
13. Yamauchi H, Fukuyama H, Nagahama Y, et al. Significance of increased oxygen extraction fraction in five-year prognosis of major cerebral arterial occlusive diseases. *J Nucl Med*. 1999; 40:1992–1998.
14. Pittman RN. Oxygen transport in normal and pathological situations: defects and compensations. In: Pittman RN, ed. *Regulation of Tissue Oxygenation*. San Rafael, CA: Morgan & Claypool Life Sciences; 2011:47–50.
15. Shahidi M, Shakoor A, Blair NP, Mori M, Shonat RD. A method for chorioretinal oxygen tension measurement. *Curr Eye Res*. 2006;31:357–366.
16. Lakowicz JR, Szmacinski H, Nowaczyk K, Berndt KW, Johnson M. Fluorescence lifetime imaging. *Anal Biochem*. 1992;202: 316–330.
17. Shonat RD, Kight AC. Oxygen tension imaging in the mouse retina. *Ann Biomed Eng*. 2003;31:1084–1096.
18. ANSI. *American National Standard for Safe Use of Lasers ANSI Z136.1-2007*. Orlando, FL: Laser Institute of America; 2007.
19. Crystal GJ. Principles of cardiovascular physiology. In: Estafanous FG, Barash PG, Reves JG, eds. *Cardiac Anesthesia: Principles and Clinical Practice*. Philadelphia, PA: Lippincott Williams & Wilkins; 2001:37–57.
20. Cartheuser CF. Standard and pH-affected hemoglobin-O2 binding curves of Sprague-Dawley rats under normal and shifted P50 conditions. *Comp Biochem Physiol Comp Physiol*. 1993;106:775–782.
21. Chen J, Edwards A, Layton AT. Effects of pH and medullary blood flow on oxygen transport and sodium reabsorption in the rat outer medulla. *Am J Physiol Renal Physiol*. 2010;298: F1369–F1383.
22. Geirsdottir A, Palsson O, Hardarson SH, Olafsdottir OB, Kristjansdottir JV, Stefansson E. Retinal vessel oxygen saturation in healthy individuals. *Invest Ophthalmol Vis Sci*. 2012; 53:5433–5442.
23. Hammer M, Vilser W, Riemer T, et al. Retinal venous oxygen saturation increases by flicker light stimulation. *Invest Ophthalmol Vis Sci*. 2011;52:274–277.
24. Hardarson SH, Harris A, Karlsson RA, et al. Automatic retinal oximetry. *Invest Ophthalmol Vis Sci*. 2006;47:5011–5016.
25. Hoffman WE, Albrecht RF, Miletich DJ. Cerebrovascular response to hypoxia in young vs aged rats. *Stroke*. 1984;15: 129–133.
26. Ito H, Kanno I, Kato C, et al. Database of normal human cerebral blood flow, cerebral blood volume, cerebral oxygen extraction fraction and cerebral metabolic rate of oxygen measured by positron emission tomography with 15O-labelled carbon dioxide or water, carbon monoxide and oxygen: a multicentre study in Japan. *Eur J Nucl Med Mol Imaging*. 2004;31:635–643.
27. Johannsson H, Siesjo BK. Cerebral blood flow and oxygen consumption in the rat in hypoxic hypoxia. *Acta Physiol Scand*. 1975;93:269–276.
28. Kobayashi M, Mori T, Kiyono Y, et al. Cerebral oxygen metabolism of rats using injectable (15)O-oxygen with a steady-state method. *J Cereb Blood Flow Metab*. 2012;32:33–40.

29. Magata Y, Temma T, Iida H, et al. Development of injectable O-15 oxygen and estimation of rat OEF. *J Cereb Blood Flow Metab*. 2003;23:671–676.
30. McPherson RW, Zeger S, Traystman RJ. Relationship of somatosensory evoked potentials and cerebral oxygen consumption during hypoxic hypoxia in dogs. *Stroke*. 1986;17: 30–36.
31. Traustason S, Jensen AS, Arvidsson HS, Munch IC, Sondergaard L, Larsen M. Retinal oxygen saturation in patients with systemic hypoxemia. *Invest Ophthalmol Vis Sci*. 2011;52: 5064–5067.
32. Hardarson SH, Stefansson E. Oxygen saturation in central retinal vein occlusion. *Am J Ophthalmol*. 2010;150:871–875.
33. Davis MJ, Hill MA, Kuo L. Local regulation of microvascular perfusion. In: Tuma RF, Duran WN, Ley K, eds. *Microcirculation*. San Diego, CA: Academic Press; 2008:161–284.
34. Harper AM, Bell RA. The effect of metabolic acidosis and alkalosis on the blood flow through the cerebral cortex. *J Neurol Neurosurg Psychiatry*. 1963;26:341–344.
35. Hermansen MC, Kotagal UR, Kleinman LI. The effect of metabolic acidosis upon autoregulation of cerebral blood flow in newborn dogs. *Brain Res*. 1984;324:101–105.
36. Ahmed J, Pulfer MK, Linsenmeier RA. Measurement of blood flow through the retinal circulation of the cat during normoxia and hypoxemia using fluorescent microspheres. *Microvasc Res*. 2001;62:143–153.
37. Nagaoka T, Sakamoto T, Mori F, Sato E, Yoshida A. The effect of nitric oxide on retinal blood flow during hypoxia in cats. *Invest Ophthalmol Vis Sci*. 2002;43:3037–3044.
38. Pournaras CJ, Rungger-Brandle E, Riva CE, Hardarson SH, Stefansson E. Regulation of retinal blood flow in health and disease. *Prog Retin Eye Res*. 2008;27:284–330.
39. Strenn K, Menapace R, Rainer G, Findl O, Wolzt M, Schmetterer L. Reproducibility and sensitivity of scanning laser Doppler flowmetry during graded changes in PO2. *Br J Ophthalmol*. 1997;81:360–364.
40. Gibbs EL, Lennox WG, Nims LF, Gibbs FA. Arterial and cerebral venous blood: arterial-venous differences in man. *J Biol Chem*. 1942;144:325–332.
41. Oshima T, Karasawa F, Satoh T. Effects of propofol on cerebral blood flow and the metabolic rate of oxygen in humans. *Acta Anaesthesiol Scand*. 2002;46:831–835.
42. McLeod D. Letter to the editor: partial central retinal artery occlusion offers a unique insight into the ischemic penumbra. *Clin Ophthalmol*. 2012;6:9–22.
43. Durukan A, Tatlisumak T. Acute ischemic stroke: overview of major experimental rodent models, pathophysiology, and therapy of focal cerebral ischemia. *Pharmacol Biochem Behav*. 2007;87:179–197.
44. Fisher M. Characterizing the target of acute stroke therapy. *Stroke*. 1997;28:866–872.
45. Heiss WD, Graf R, Grond M, Rudolf J. Quantitative neuroimaging for the evaluation of the effect of stroke treatment. *Cerebrovasc Dis*. 1998;8:23–29.